

1 **Efficacy, safety, and biomarker analyses of bintrafusp alfa, a bifunctional fusion**
2 **protein targeting TGF- β and PD-L1, in patients with advanced non-small cell lung**
3 **cancer**

4 **Authors:** Arun Rajan, MD,¹ Houssein Abdul Sater, MD,² Osama Rahma, MD,³ Richy
5 Agajanian, MD,⁴ Wiem Lassoued, PhD,⁵ Jennifer Marté, MD,⁶ Yo-Ting Tsai, PhD,⁵ Renee N.
6 Donahue, PhD,⁵ Elizabeth Lamping RN,⁶ Shania Bailey, BS,⁷ Andrew Weisman, PhD,⁸ Beatriz
7 Walter Rodriguez, MD, PhD,⁹ Rena Ito, MD, PhD,¹⁰ Yulia Vugmeyster, PhD,¹¹ Masashi Sato,
8 MSc,¹⁰ Andreas Machl, PhD,¹¹ Jeffrey Schlom, PhD,⁵ James L. Gulley MD, PhD,⁵

9

10 **SUPPLEMENTARY MATERIALS**

11

12 **Section A.** Details of the treatment procedures and statistical analyses.

13 **Section B.** Details of biomarker methodologies.

14 **List of Supplementary Tables and Figures**

15 **Supplementary Table 1:** Details of the antibodies, protocols, and Opal kits used.

16 **Supplementary Table 2.** Baseline and disease characteristics of biomarker-evaluable patients

17 **Supplementary Table 3.** Baseline patient PD-L1 expression based on various cut-off points in
18 non-biomarker evaluable patients

19 **Supplementary Table 4:** Efficacy according to Response Evaluation Criteria in Solid Tumors
20 1.1 as assessed by the investigator.

21

22 **Supplementary Table 5.** Patients reporting adverse events of special interest.

23 **Supplementary Table 6.** Changes in the peripheral immune profile of patients after one, three,
24 and six cycles of therapy. Changes in (A) soluble analytes, (B) complete blood counts, and (C)
25 PBMC immune subsets before and during treatment 15, 43, and 85 days after the initiation of
26 bintrafusp alfa.

27 **Supplementary Figure 1.** Differences in the peripheral immune profile of patients who were
28 ICI-naïve vs. ICI-experienced. Baseline levels of (A) soluble analytes (measured by enzyme-
29 linked immunosorbent and Olink assay), (B) complete blood counts, and (C) PBMC immune cell
30 subsets (measured by flow cytometry) that were different between patients who were ICI-naïve
31 (n=6) and ICI-experienced (n=8) before treatment with bintrafusp alfa. (D) Changes in PBMC
32 immune subsets after one cycle of therapy (D15) vs. baseline that were different between

33 patients who were ICI-naïve and those who were ICI-experienced before treatment with
34 bintrafusp alfa.

35 **Supplementary Figure 2.** The peripheral immune profile of patients pre- and on-treatment with
36 bintrafusp alfa associates with clinical response as measured by BOR. Baseline levels (A) and
37 early changes after (B) 1 cycle (day 15 vs. pre), (C) 2 cycles (day 29 vs. pre), and (D) 3 cycles
38 (day 43 vs. pre) of bintrafusp alfa in soluble analytes and complete blood counts that associate
39 with BOR.

40 **Supplementary Figure 3.** Representative hematoxylin and eosin showing fibrosis on-treatment
41 with bintrafusp alfa. (A) Pre-treatment biopsy shows a moderately differentiated
42 adenocarcinoma. (B) On-treatment tumor biopsy from the same patient highlights areas of
43 fibrosis and inflammation. H&E images were scanned at 20X resolution.

44 **Supplementary Figure 4.** Changes in immune cell profiles in the tumor microenvironment of
45 patients pre- and on-treatment with bintrafusp alfa were grouped by PFS (<3 months vs. >3
46 months). (A) Each pie chart shows percentages of various immune subsets in biopsies from each
47 patient pre-treatment (designated as A for each patient number) and on-treatment (designated as
48 B for each patient number) with bintrafusp alfa. (B) Representative 20X images of paired biopsy
49 tissues from two patients (#507 and #510) immuno-stained with the multiplex IF-panel.
50

51 **Section A. Details of the treatment procedures and statistical analysis**

52 **Treatment procedures**

53 Premedication with an antihistamine and acetaminophen (administered 30–60 min before
54 each dose of bintrafusp alfa) was optional for all infusions to mitigate potential infusion-related
55 reactions; steroids were not permitted as premedication. Dose reduction was not permitted, and
56 interruption or discontinuation of bintrafusp alfa was allowed if treatment-related adverse events,
57 infusion-related reactions of grade ≥ 2 severity, or severe or life-threatening adverse events (AEs)
58 occurred.

59 Tumor response was assessed by radiographic imaging using RECIST version 1.1 6
60 weeks after starting treatment, then every 6 weeks for the first year and every 12 weeks
61 thereafter. Response was confirmed by repeated radiographic assessment 4 weeks or longer from
62 the first documented response. To evaluate the safety of bintrafusp alfa, AEs were monitored

63 throughout treatment and assessed using CTCAE version 4.03 at 28 days after the last study
64 dose, at 10 weeks post-treatment, and every 12 weeks thereafter.

65 **Statistical analysis**

66 The uncertainty of the estimates was assessed by calculating a 95% exact (Clopper–
67 Pearson) confidence interval. The disease control rate was defined as the proportion of patients
68 with a confirmed best overall response (BOR) of complete response (CR), partial response (PR),
69 stable disease (SD), or non-CR/nonprogressive disease. The duration of response was analyzed
70 using Kaplan–Meier analysis as were progression-free survival (PFS) and overall survival.
71 Safety and pharmacokinetic parameters were analyzed using descriptive statistics. PK parameters
72 after the first dose, including concentration after the end of infusion (C_{eoi}), area under the serum
73 concentration–time curve, clearance, and half-life, were derived via noncompartment analysis.
74 Furthermore, C_{eoi} and C_{trough} were obtained throughout the treatment period (reported as
75 geometric mean with geometric coefficient variation percentage).

76

77 **Section B. Details of biomarker methodologies**

78 Programmed death ligand 1 tumor cell expression was determined using different
79 immunohistochemistry assays, such as antibody clone 73-10, E1L3N, 22C3 (DAKO FDA-
80 approved pharmDx™ protocol using the DAKO automated link 48 platform) [1-3], VENTANA
81 PD-L1 (SP263) [4], and clone SP142 from Abcam (catalog ab228463) using the Leica Bond
82 Max platform. The peripheral immunome of patients (n = 14) with non-small cell lung cancer
83 enrolled at the National Cancer Institute (NCI) was analyzed before treatment with bintrafusp
84 alfa and at 2 (after 1 cycle), 4 (after 2 cycles), 6 (after 3 cycles), and 12 (after 6 cycles) weeks
85 after therapy initiation, where samples were available. Patients were analyzed for levels and

86 changes in (a) multiple serum and plasma soluble factors, including analytes reflecting immune
87 stimulatory and inhibitory status, (b) complete blood counts, and (c) 158 immune cell subsets.
88 For the analyses of peripheral immune parameters with clinical response, patients with a PFS of
89 >3 months (n = 8) were compared with those with a PFS of <3 months (n = 6). Analyses were
90 also performed by comparing patients with a BOR of CR or PR (n = 3) with those with a BOR of
91 SD (n = 9) or progressive disease (PD) (n = 2). Analyses were also performed by comparing the
92 peripheral immune profile of immune checkpoint inhibitor (ICI)-naïve patients (n = 6) with that
93 of ICI-experienced patients (n = 8) and of patients with a history of heavy smoking (n = 10) with
94 that of nonsmokers (n = 4).

95 Complete blood counts with differential analysis were performed at the NCI's Center for
96 Cancer Research, and the neutrophil-to-lymphocyte ratio was subsequently calculated. For serum
97 assays, blood was collected in serum separator tubes, centrifuged, and stored at -80°C before
98 analysis. For plasma assays, blood was collected in ethylenediaminetetraacetic acid tubes,
99 centrifuged, and stored at -80°C before analysis. For the analysis of peripheral blood
100 mononuclear cells (PBMCs), blood was collected in sodium heparin tubes, and PBMCs were
101 isolated after Ficoll–Hypaque density gradient separation. Cells were cryopreserved in 90% heat-
102 inactivated human AB serum and 10% dimethyl sulfoxide at a concentration of 1×10^7 cells/mL
103 before analysis.

104 The serum levels of IL-8, sCD27, sCD40L, and sPD-L1 and plasma levels of sPD-1,
105 sCD73, TGF- β 1, and Granzyme B were analyzed using commercially available kits according to
106 the manufacturers' instructions. IL-8 was measured using AlphaLISA (PerkinElmer, Waltham,
107 MA, USA); sCD27 and sCD40L were measured using instant enzyme-linked immunosorbent
108 assay (ELISA) kits (Life Technologies, Carlsbad, CA, USA); sPD-1, sPD-L1, and sCD73 were

109 measured using ELISA kits from Abcam (Cambridge, UK); and TGF- β 1 and Granzyme B were
110 measured using ELISA kits from R&D Systems (Minneapolis, MN, USA). Plasma samples were
111 also analyzed using Olink Target 96 Immuno-Oncology panel for biomarker discovery (Olink,
112 Watertown, MA, USA).

113 Cryopreserved PBMCs collected before and after bintrafusp alfa therapy were examined
114 via multicolor flow cytometry using 30 markers in four panels to identify 158 peripheral immune
115 cell subsets[5] following methods previously described.[6,7] The subsets evaluated included 10
116 parental cell types (CD4⁺ and CD8⁺ T cells, regulatory T cells, NK cells, NKT cells,
117 conventional dendritic cells, plasmacytoid dendritic cells, B cells, myeloid-derived suppressor
118 cells, and monocytes) and 148 refined subsets related to the maturation/function of the parental
119 cell types. Flow cytometry files were acquired on an LSR Fortessa equipped with five lasers and
120 analyzed using FlowJo v.9.9.6 for Macintosh, with nonviable cells excluded and negative gates
121 based on fluorescence-minus-one controls. The frequency of all subsets was calculated as a
122 percentage of PBMCs to eliminate any bias that might occur in the smaller populations with
123 fluctuations in parental leukocyte populations.

124 Multiplex immunofluorescence staining and multispectral imaging: Formalin-fixed
125 paraffin-embedded 5- μ m sections from tumor biopsies were immunostained using Opal
126 multiplex 6-plex kits according to the manufacturer's protocol (Akoya Biosciences) for a panel
127 of DAPI, CD4, CD8, FOXP3, CD56, CD68, and CD163. Deparaffinization, rehydration, epitope
128 retrieval, and staining of slides were performed using Leica BOND RX Autostainer (Leica). The
129 optimum staining conditions for each antibody were determined using IHC and single
130 immunofluorescence before combination. Details regarding the antibodies, protocols, and opals
131 used in this panel are described in Supplementary Table 1. Hematoxylin and eosin and multiplex

132 immunofluorescence whole-slide scans were captured using Vectra Polaris (PerkinElmer) at 20x
133 magnification. Selected regions of interest (ROI) were scanned at 40x magnification for
134 multispectral (MS) imaging. MS images were unmixed and analyzed using InForm, version 2.5
135 (Akoya Biosciences). Using training ROI images, an algorithm was built and applied for cell
136 segmentation and phenotyping. All immune cell infiltrates were measured as cell counts/mm² of
137 tissue (density).

138 T-cell receptor (TCR) sequencing: TCR sequencing of biopsy tissue obtained before and during
139 treatment (~7 weeks after treatment initiation) was performed using the Adaptive
140 Biotechnologies immunoSEQ assay where adequate samples were available (n = 9). Eight
141 samples were fresh-frozen cores; one was formalin-fixed, paraffin-embedded tissue. TCR-seq
142 was also performed on the corresponding PBMCs. The number of clones comprising the top
143 25% of the T-cell repertoire were analyzed, and their associations with the BOR were
144 investigated.

145 **Supplementary references:**

- 146 1. Grote HJ, Feng Z, Schlichting M, et al. Programmed death-ligand 1
147 immunohistochemistry assay comparison studies in NSCLC: characterization of the 73-
148 10 assay. *J Thorac Oncol.* 2020;15:1306–1316.
- 149 2. Munari E, Zamboni G, Lunardi G, et al. PD-L1 expression in non-small cell lung cancer:
150 evaluation of the diagnostic accuracy of a laboratory-developed test using clone E1L3N
151 in comparison with 22C3 and SP263 assays. *Hum Pathol.* 2019;90:54–59.
- 152 3. Torous VF, Rangachari D, Gallant BP, Shea M, Costa DB, VanderLaan PA. PD-L1
153 testing using the clone 22C3 pharmDx kit for selection of patients with non-small cell

- 154 lung cancer to receive immune checkpoint inhibitor therapy: are cytology cell blocks a
155 viable option? *J Am Soc Cytopathol.* 2018;7:133–141.
- 156 4. Ventana PD-L1 (SP263) Assay. CE marked package insert. Roche Diagnostics; 2022.
- 157 5. Donahue RN, Marté JL, Goswami M, et al. Interrogation of the cellular immunome of
158 cancer patients with regard to the COVID-19 pandemic. *J Immunother Cancer.*
159 2021;9:e002087.
- 160 6. Lepone LM, Donahue RN, Grenga I, et al. Analyses of 123 peripheral human immune
161 cell subsets: defining differences with age and between healthy donors and cancer
162 patients not detected in analysis of standard immune cell types. *J Circ Biomark.* 2016;5:5.
- 163 7. Donahue RN, Lepone LM, Grenga I, et al. Analyses of the peripheral immunome
164 following multiple administrations of avelumab, a human IgG1 anti-PD-L1 monoclonal
165 antibody. *J Immunother Cancer.* 2017;5:20.

166 **Supplementary Table 1:** Details of the antibodies, protocols, and Opal kits used

Antibody	Clone	Catalog#	Company	Dilution	ER (Leica)	Secondary antibody (Vector labs)	OPAL (Akoya Biosciences)
CD68	D4B9C	76437	Cell signaling	1:400	ER1	Immpress Mouse/Rabbit	520 (FP1487001KT)
CD4	EPR6855	ab133616	Abcam	1:250	ER1	Immpress Mouse/Rabbit	570 (FP1488001KT)
CD8	EPR10640	ab215041	Abcam	1:100	ER1	Immpress Mouse/Rabbit	540 (FP1494001KT)
FOXP3	SP97	MA5-16365	Thermo-Fisher	1:200	ER2	Immpress Mouse/Rabbit	620 (FP1495001KT)
CD163	EPR19518	ab182422	Abcam	1:200	ER2	Immpress Mouse/Rabbit	650 (FP1496001KT)
CD56	MRQ-42	156R-94	Sigma-Aldrich	1:200	ER2	Immpress Mouse/Rabbit	690 (FP1497001KT)

167 CD4/8/56/68/163; cluster of differentiation 4/8/56/68/163; FOXP3, forkhead box P3

168

169

170

171

172

173

174

175

176

177

178

179

180

181

182

183

184

185 **Supplementary Table 2.** Baseline and disease characteristics in biomarker-evaluable patients

Characteristics, n (%)	Biomarker-evaluable cohort	
	ICI-naïve (n = 6)	ICI-experienced (n = 8)
Sex		
Male	2 (33.3)	5 (62.5)
Female	4 (66.7)	3 (37.5)
Age		
Median (range), years	60.5 (50–73)	58.5 (52–73)
<65 years	4 (66.7)	5 (62.5)
≥65 years	2 (33.3)	3 (37.5)
ECOG performance status		
0	1 (16.7)	0
1	5 (83.3)	8 (100.0)
Tumor cell PD-L1 expression^a		
<1%	2 (33.0)	1 (12.5)
1–49%	1 (16.7)	1 (12.5)
50–75%	0	1 (12.5)
>75%	1 (16.7)	1 (12.5)
Not available	2 (34.0)	4 (50.0)
EGFR mutation status^b		
Wild type	4 (66.6)	6 (85.7)
Mutated	1 (16.7)	1 (14.3)
Not available	1 (16.7)	0
Tumor histology		
Adenocarcinoma	5 (83.3)	6 (75.0)
Squamous cell carcinoma	0	1 (12.5)
Other	1 (16.7)	1 (12.5)
Number of prior anticancer regimens		
0	3 (50.0)	0
1	1 (16.7)	0
2	0	5 (62.5)
3	0	2 (25.0)
≥4	2 (33.3)	1 (12.5)
Type of prior anticancer therapy for metastatic or locally advanced disease		
Anti-PD-(L)1	0	7 (87.5)
Cytotoxic therapy	2 (33.3)	5 (62.5)
Endocrine therapy	0	0
Monoclonal antibody therapy	0	3 (37.5)
Small molecules	2 (33.3)	1 (12.5)
Immunotherapy other than anti-PD-(L)1	1 (16.7)	1 (12.5)
Other	0	0

186 ECOG, Eastern Cooperative Oncology Group; ICI, immune checkpoint inhibitor; PD-L1, programmed cell death ligand 1.

187 Data are presented as n (%) or median (range)

188 ^a PD-L1 immunohistochemistry data were obtained using one of the following clones: 73-10, clone E1L3N, clone SP263, and

189 clone 22C3.

190 ^bThe percentage is calculated based on the number of subjects with nonsquamous histology.

191

192

193 **Supplementary Table 3:** Baseline patient PD-L1 expression based on various cut-off points in
 194 non-biomarker evaluable patients

195

Tumour cell PD-L1 expression ^{a,b}	ICI-naïve (n = 12)	ICI-experienced (n = 15)
≥10%	3 (25.0)	5 (33.3)
<10%	7 (58.3)	9 (60.0)
Not available	2 (16.7)	1 (6.7)
≥20%	3 (25.0)	5 (33.3)
<20%	7 (58.3)	9 (60.0)
Not available	2 (16.7)	1 (6.7)
≥50%	2 (16.7)	4 (26.7)
<50%	8 (66.7)	10 (66.7)
Not available	2 (16.7)	1 (6.7)
≥80%	1 (8.3)	2 (13.3)
<80%	9 (75.0)	12 (80.0)
Not available	2 (16.7)	1 (6.7)

196 ICI, immune checkpoint inhibitor; PD-L1, programmed cell death ligand 1; TPS, tumor proportion score.

197 ^aFor 27 patients the calculated scorings for TPS ≥10%, ≥20%, ≥50% and ≥80% are based on a continuous reading of the TPS for
 198 1+, 2+ and 3+ tumor cells. A TPS has been calculated by summing up the TPS scores for 1+, 2+ and 3+ tumor cells. Based on the
 199 calculated TPS score the samples were classified as negative/positive for TPS ≥10%, ≥20%, ≥50% and ≥80% based on the
 200 respective cut-point.

201 ^bPD-L1 immunohistochemistry data were obtained using the clone 73-10.

202

203

204

205

206

207

208

209

210

211

212

213

214

215

216

217 **Supplementary Table 4.** Efficacy according to RECIST 1.1 as assessed by the investigator

	ICI-naïve (n = 18)	ICI-experienced (n = 23)
Confirmed BOR		
Complete response (CR)	1 (5.6)	0
Partial response (PR)	4 (22.2)	0
Stable disease (SD)	5 (27.8)	5 (21.7) ^a
Progressive disease (PD)	4 (22.2)	13 (56.5) ^b
Not evaluable	4 (22.2)	5 (21.7)
Overall response rate (CR+PR), (95% CI)	5 (27.8) (9.7–53.5)	0 (0.0–14.8)
Disease control rate (95% CI)	10 (55.6) (30.8–78.5)	5 (21.7) ^a (7.5–43.7)
Median progression-free survival, months (95% CI)	2.8 (1.4–6.5)	1.4 (1.3–1.4)
Median duration of response, months (95% CI)	16.8 (2.8–NE)	NE (NE–NE)

218 BOR, best overall response; CI, confidence interval; ICI, immune checkpoint inhibitor; IRC, independent review committee; NE,
219 not estimable; RECIST, Response Evaluation Criteria in Solid Tumors

220 Data are presented as n (%) and n (%; 95% CI), unless specified otherwise.

221 ^aAmong the five patients with SD, three had stable disease at the initial tumor evaluation in week 6, which changed to
222 progressive disease in the subsequent evaluation. The sum of the longest diameter at the initial tumor evaluation showed an
223 increase of 19.9%, 19.5%, and 19.7% for these patients compared with the baseline measurements.

224 ^bTwo cases of radiological pseudoprogression showed progressive disease at the first restaging, and on subsequent scans, they
225 showed stable disease or partial response.

226

227 **Supplementary Table 5.** Patients reporting adverse events of special interest

	ICI-naïve (n = 18)		ICI-experienced (n = 23)	
	Any grade, n (%)	Grade ≥3, n (%)	Any grade, n (%)	Grade ≥3, n (%)
Immune-related AESI	3 (16.7)	0	4 (17.4)	1 (4.3)*
Immune-related endocrinopathies: adrenal insufficiency	1 (5.6)	0	1 (4.3)	1 (4.3)*
Adrenal insufficiency	1 (5.6)	0	1 (4.3)	1 (4.3)*
Immune-related rash	2 (11.1)	0	2 (8.7)	0
Lichen planus	1 (5.6)	0	-	-
Pruritus	2 (11.1)	0	1 (4.3)	0
Rash	-	-	1 (4.3)	0
Immune-related endocrinopathies: thyroid disorders	-	-	1 (4.3)	0
Hypothyroidism	-	-	1 (4.3)	0
Skin AESI	4 (22.2)	-	5 (21.7)	-
Keratoacanthoma	3 (16.7)	-	3 (13.0)	-
Squamous cell carcinoma of skin	1 (5.6)	-	0	-
Hyperkeratosis	0	-	1 (4.3)	-
Actinic keratosis	0	-	1 (4.3)	-

228 *Also reported as grade ≥4 events.

229 AESI, adverse events of special interest; ICI, immune checkpoint inhibitor

230

231 **Supplementary Table 6.** Changes in the peripheral immune profile of patients after one, three,
232 and six cycles of therapy

A

Soluble Analyte	Change	Timepoint 1					Timepoint 2					Timepoint 3				
		Median D1	Median D15	P value	% with $\geq 25\%$ increase	% with $\geq 25\%$ decrease	Median D1	Median D43	P value	% with $\geq 25\%$ increase	% with $\geq 25\%$ decrease	Median D1	Median D85	P value	% with $\geq 25\%$ increase	% with $\geq 25\%$ decrease
sCD27	↑	62.3	77.6	0.068	50	0	62.3	86.8	0.077	50	8	62.4	95.4	0.020	78	0
sCD27/sCD40L	↑	5.1	6.3	0.042	57	14	4.5	5.8	0.151	50	8	4.4	8.3	0.055	78	11
TGF β	↓	68247	1673	<0.001	0	100	63510	1385	0.001	0	100	71714	1444	0.002	0	100
CCL17	↑	11.27	11.88	0.049	57	7										

B

Complete Blood Count	Change	Timepoint 1					Timepoint 2					Timepoint 3				
		Median D1	Median D15	P value	% with $\geq 25\%$ increase	% with $\geq 25\%$ decrease	Median D1	Median D43	P value	% with $\geq 25\%$ increase	% with $\geq 25\%$ decrease	Median D1	Median D85	P value	% with $\geq 25\%$ increase	% with $\geq 25\%$ decrease
White Blood	↑	7.2	8.4	0.006	57	0	7.2	7.6	0.080	31	0	7.2	6.7	0.123	55	9
Neutrophil	↑	4.5	5.9	0.002	57	0	4.4	4.9	0.092	46	8	3.8	4.5	0.206	55	9

C

PBMC Subset	Change	Timepoint 1					Timepoint 2					Timepoint 3				
		Median D1	Median D15	P value	% with $\geq 25\%$ increase	% with $\geq 25\%$ decrease	Median D1	Median D43	P value	% with $\geq 25\%$ increase	% with $\geq 25\%$ decrease	Median D1	Median D85	P value	% with $\geq 25\%$ increase	% with $\geq 25\%$ decrease
CD8	↓	11.5	9.4	0.049 ^A	14	36	11.3	7.5	0.021	8	67	13.1	6.3	0.049	10	70
NK-T	↓	1.7	0.9	0.025	7	64	1.7	1.1	0.021	8	67	1.7	1.0	0.193	20	50
B cells	↑	9.8	11.3	0.268	36	7	11.4	15.4	0.021	58	0	11.4	13.7	0.131	50	10
cDC	↑	0.3	0.4	0.217	64	14	0.3	0.5	0.001	75	0	0.3	0.4	0.020	70	10
pDC	↑	0.10	0.13	0.030	57	14	0.10	0.12	0.021	75	0	0.1	0.1	0.275	60	30
MDSC	↑	7.8	8.9	0.030	64	7	6.7	5.6	0.733	42	33	7.8	12.0	0.084	50	10
Monocytes	↑	22.0	26.8	0.035 ^A	43	0	18.7	23.2	0.052	33	0	22.0	28.8	0.049	50	0
EM CDB	↓	4.07	3.05	0.030	14	50	3.46	2.18	0.005	8	92	4.07	1.69	0.065	10	80
Ki67 + CDB	↓	0.26	0.17	0.020	21	57	0.26	0.10	0.021	17	67	0.30	0.18	0.301	33	67

233

234 Changes in (A) soluble analytes, (B) complete blood counts, and (C) PBMC immune subsets
235 before and during treatment 15, 43, and 85 days after the initiation of bintrafusp alfa. Changes in
236 immune parameters between two timepoints were calculated using Wilcoxon signed-rank test.
237 Units shown in A are U/mL for sCD27, pg/mL for TGF β , and NPX for CCL17. Units shown are
238 K/ μ L in B and % of PBMC in C. ^ADespite significant *p*-values, most patients did not exhibit a
239 >25% change. CD, cluster of differentiation; CCL17, CC motif chemokine ligand 17; cDC,
240 conventional dendritic cells; D, days; EM, effector memory; MDSC, myeloid-derived suppressor
241 cells; NKT, natural killer T cells; NPX, normalized protein expression; PBMC, peripheral blood
242 mononuclear cells; pDC, plasmacytoid dendritic cells; TGF- β , transforming growth factor-beta;
243 sCD27/sCD40L, soluble CD27/soluble CD40 ligand.

244

245

246 **Supplementary Figure 1.** Differences in the peripheral immune profile of patients who were
247 ICI-naïve vs. ICI-experienced. Baseline levels of (A) soluble analytes (measured via enzyme-
248 linked immunosorbent and Olink assays), (B) complete blood counts, and (C) PBMC immune
249 subsets (measured via flow cytometry) that were different between patients who were ICI-naïve
250 (n = 6) and those who were ICI-experienced (n = 8) before treatment with bintrafusp alfa. (D)
251 Changes in PBMC immune subsets after one cycle of therapy (D15) vs. baseline that were
252 different between patients who were ICI-naïve and those who were ICI-experienced before
253 treatment with bintrafusp alfa. Graphs display the median frequency of analytes, and *p*-values
254 were calculated using Mann–Whitney test. B cell, bursa-derived cells; CD, cluster of
255 differentiation; D, day; EM, effector memory; EMRA, terminally differentiated effector
256 memory; ICI, immune checkpoint inhibitor; IL-10, interleukin-10; NPX, normalized protein
257 expression; NLR, neutrophil-to-lymphocyte ratio; PBMC, peripheral blood mononuclear cell;
258 sPD-1/sPD-L1, soluble programmed death-1/ligand-1; Treg, regulatory T cells.

259

260

261

262

263

264

265

266

267

268

269

270

271

272

273

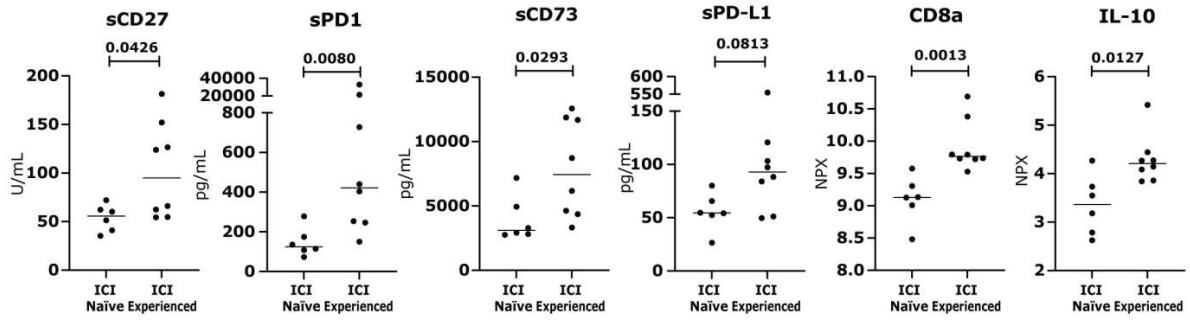
274

275

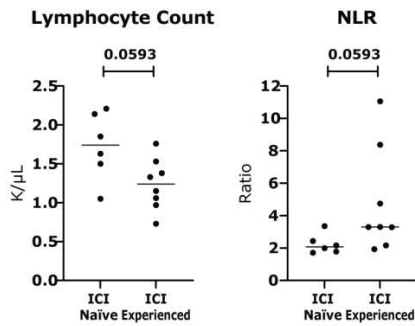
276

277

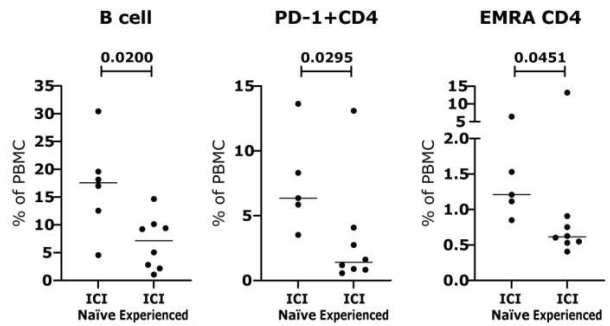
A Baseline: Soluble Analytes



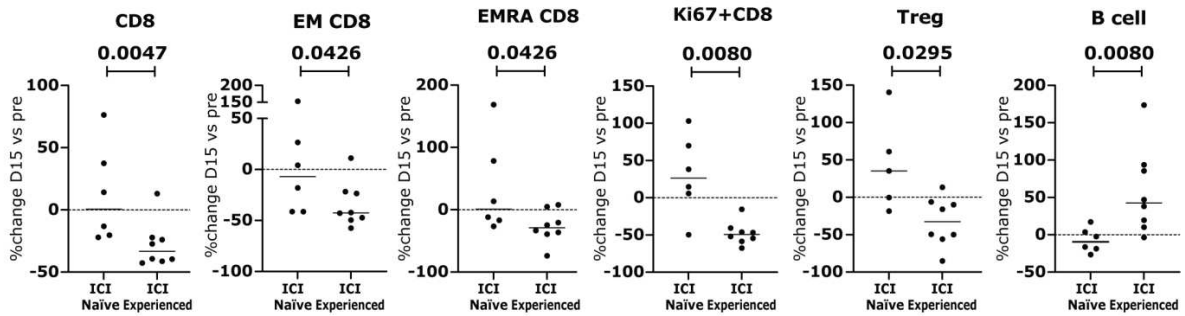
B Baseline: Complete Blood Counts



C Baseline: PBMC Subsets



D Change (D15 vs Pre): PBMC Subsets

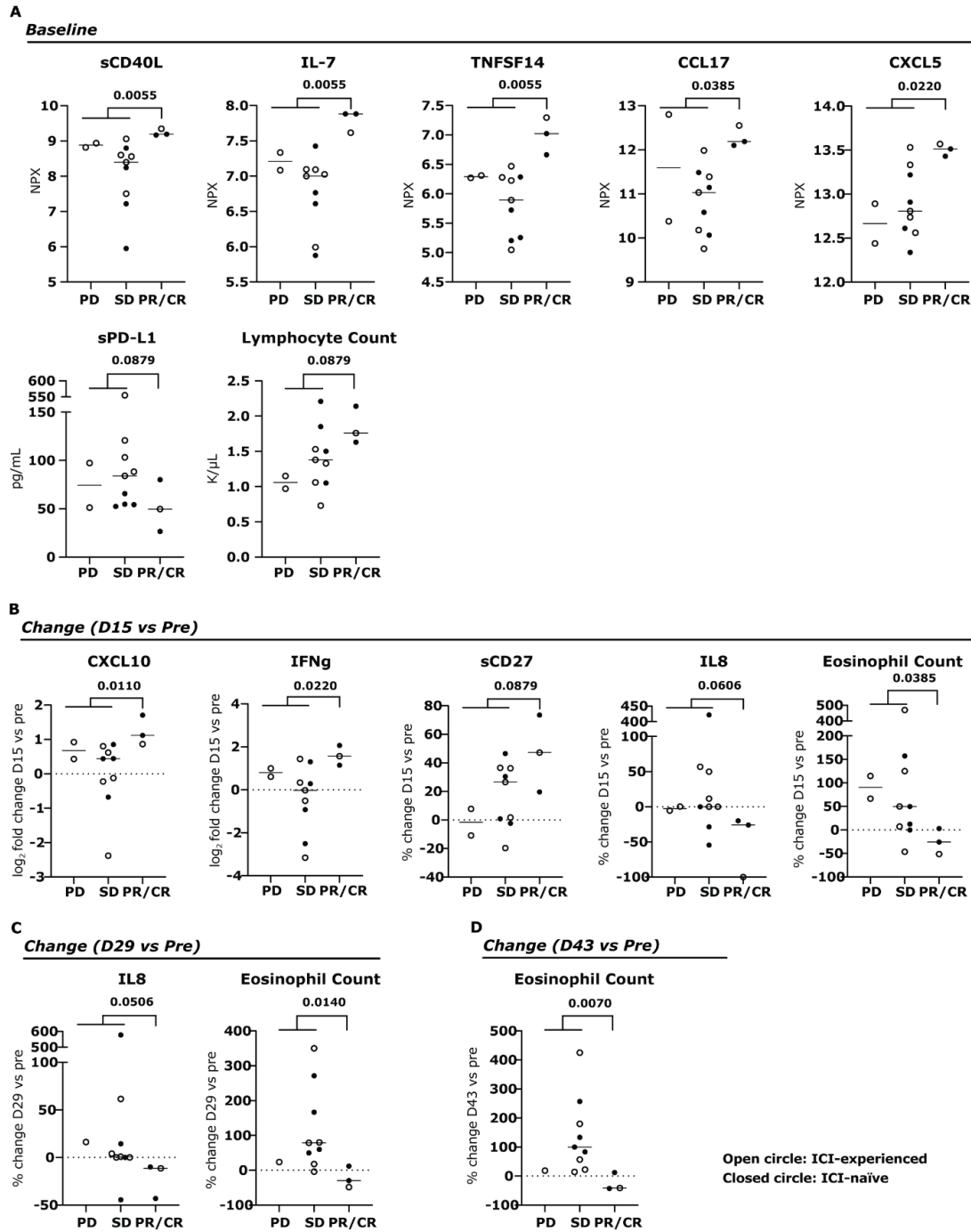


279 **Supplementary Figure 2.** The peripheral immune profile of patients pre- and on-treatment with
280 bintrafusp alfa associates with clinical response as measured by BOR. Baseline levels (A) and
281 early changes after (B) 1 cycle (day 15 vs. pre), (C) 2 cycles (day 29 vs. pre), and (D) 3 cycles
282 (day 43 vs. pre) of bintrafusp alfa in soluble analytes and complete blood counts that associate
283 with BOR. Patients with BOR of CR or PR (n = 3) were compared to those with a BOR of PD (n
284 = 2) and SD (n = 9). Graphs display median frequency of analytes and *p* values were calculated
285 using the Mann-Whitney test. BOR, best overall response; CCL17, C-C motif ligand 17; CD,
286 cluster of differentiation; CR, complete response; CXCL5/10, C-X-C motif chemokine ligand
287 5/10; D, day; IFN- γ , interferon-gamma; IL-7/8, interleukin 7/8; NPX, normalized protein
288 expression; PD, progressive disease; PR, partial response; SD, stable disease; s, soluble; sPD-
289 1/sPD-L1, soluble programmed death-1/ligand-1; TNFSF14, tumor necrosis factor superfamily
290 member 14.

291

292

293

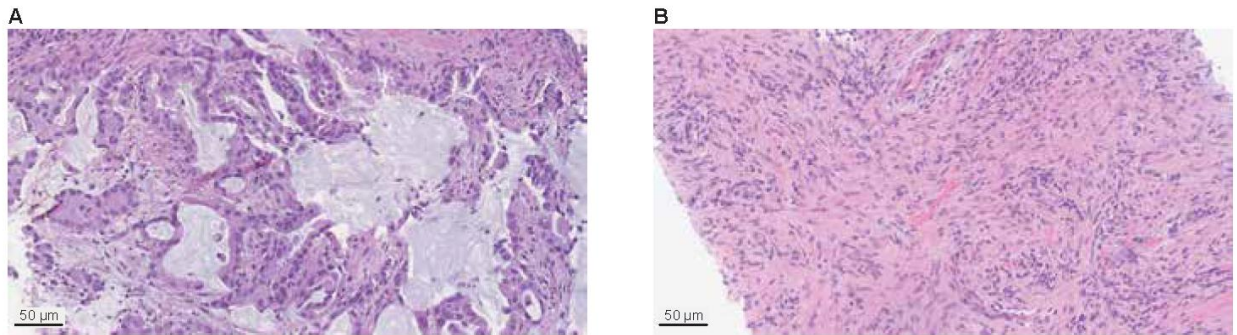


294

295

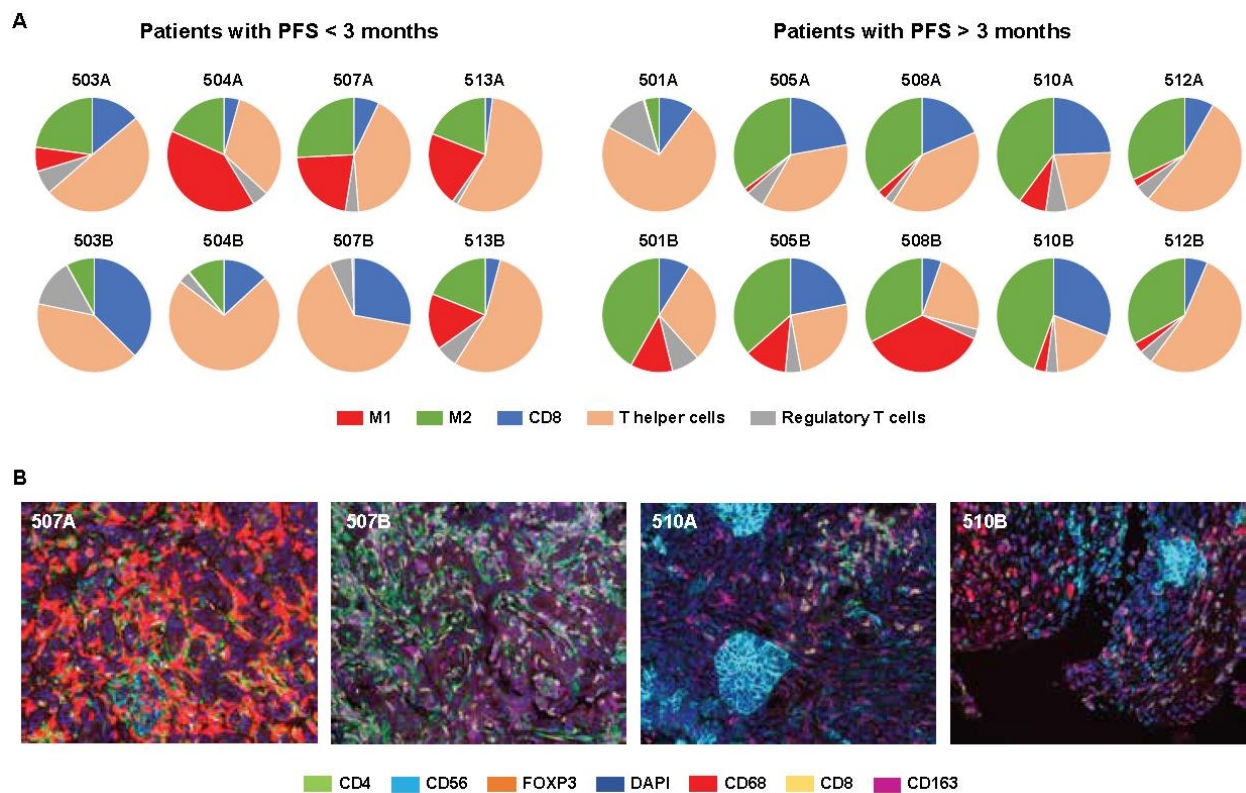
296 **Supplementary Figure 3.** Representative hematoxylin and eosin showing fibrosis on-treatment
297 with bintrafusp alfa. (A) Pre-treatment biopsy shows a moderately differentiated
298 adenocarcinoma. (B) On-treatment tumor biopsy from the same patient highlights areas of
299 fibrosis and inflammation. H&E images were scanned at 20X resolution. H & E, hematoxylin
300 and eosin.

301



303 **Supplementary Figure 4.** Changes in immune cell profiles in the tumor microenvironment of
 304 patients pre- and on-treatment with bintrafusp alfa were grouped by PFS (<3 months vs. >3
 305 months). (A) Each pie chart shows percentages of various immune subsets in biopsies from each
 306 patient pre-treatment (designated as A for each patient number) and on-treatment (designated as
 307 B for each patient number). (B) Representative 20X images of paired biopsy tissues from two
 308 patients (#507 and #510) immuno-stained with the multiplex IF-panel (CD4, CD8, CD68, CD56,
 309 CD163, FOXP3 and DAPI) are shown. CD, cluster of differentiation 4/8/56/68/163; DAPI, 4',6-
 310 diamidino-2-phenylindole; FOXP3, forkhead box P3; M1, inflammatory macrophages; M2,
 311 tumor-tropic macrophages; PFS, progression-free survival; IF-panel, immunofluorescence-
 312 panel.

313
 314
 315



316